Electronic Supplementary Information

Metal Intercalation Induced Magnetic Modulation in VS_2 Bilayer: A First Principles Study

Dantong Li, Xiaocheng Zhou, Yu Wang, and Yafei Li**

Key Laboratory of Numerical Simulation for Large Scale Complex Systems (Ministry of Education of PRC), School of Chemistry and Materials Science, Nanjing Normal University, Nanjing 210023, China

To whom correspondence should be addressed. Email: xczhou@njnu.edu.cn (XZ) and liyafei@njnu.edu.cn (YL)

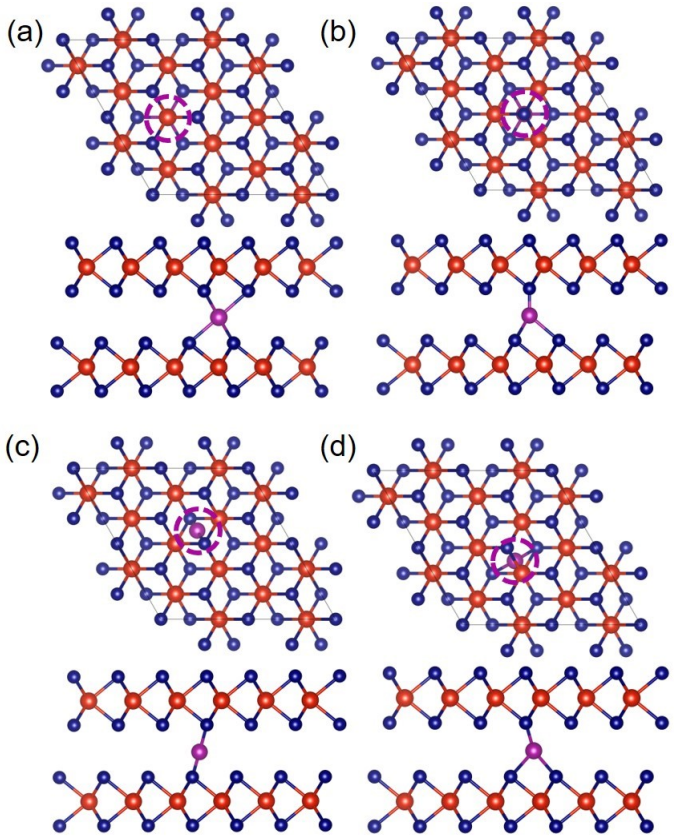

Fig. S1 Four kinds of possible positions of the intercalated TM atoms, (a) octahedral, (b) tetrahedral, (c-d) two hollow positions.

We systematically investigated possible intercalation sites for transition metals (TMs) in the van der Waals (vdW) gap of VS_2 bilayer. Using the 1Cr-VS_2 as an example, four distinct interstitial sites, including octahedral (A), tetrahedral (B), and two hollow positions (C and D), were evaluated (Fig. S1). Notably, D configuration spontaneously relaxed into the octahedral coordinated structure during geometry optimization. Therefore, we discussed total energies of A-C configurations.

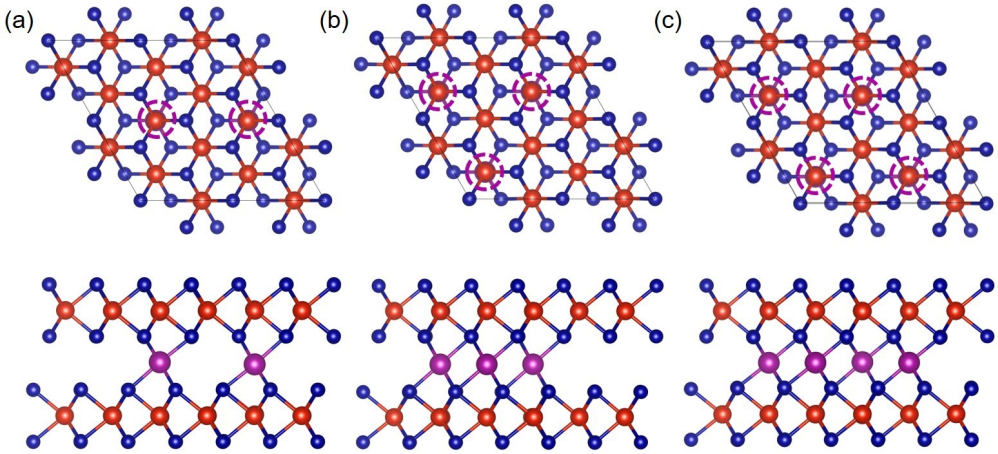

Fig. S2 Top and side views of TM-VS_2 at the intercalation concentrations of (a) 16.7%, (b) 25%, (c) 33.3%.

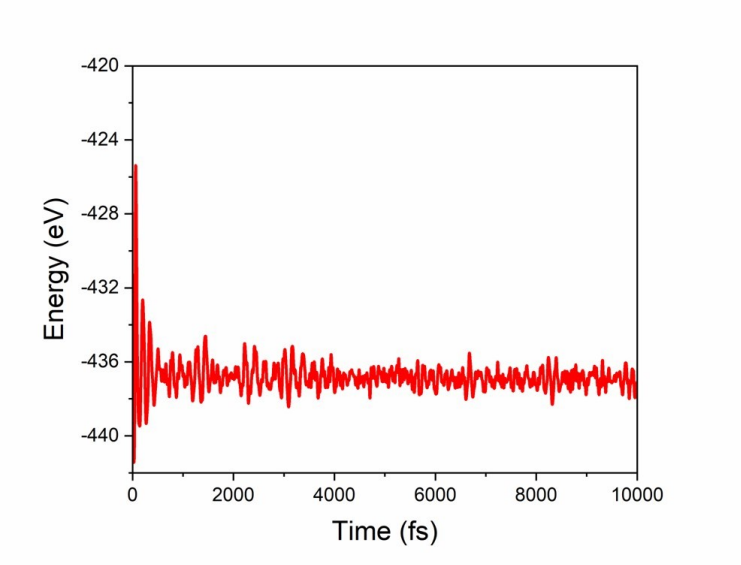

Fig. S3 The energy evolution during the AIMD simulations for 4Cr-VS_2 system. The AIMD simulations last for 10 ps at 500 K.

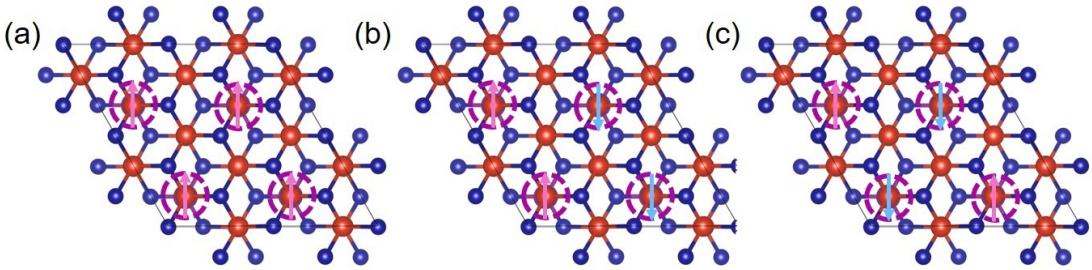

Fig. S4 Schematics of four different magnetic structures for 4TM-VS_2 system: (a) FM, (b) AFM1, (c) AFM2, where pink arrows represent the spin up configurations and blue arrows represent the spin down configurations.

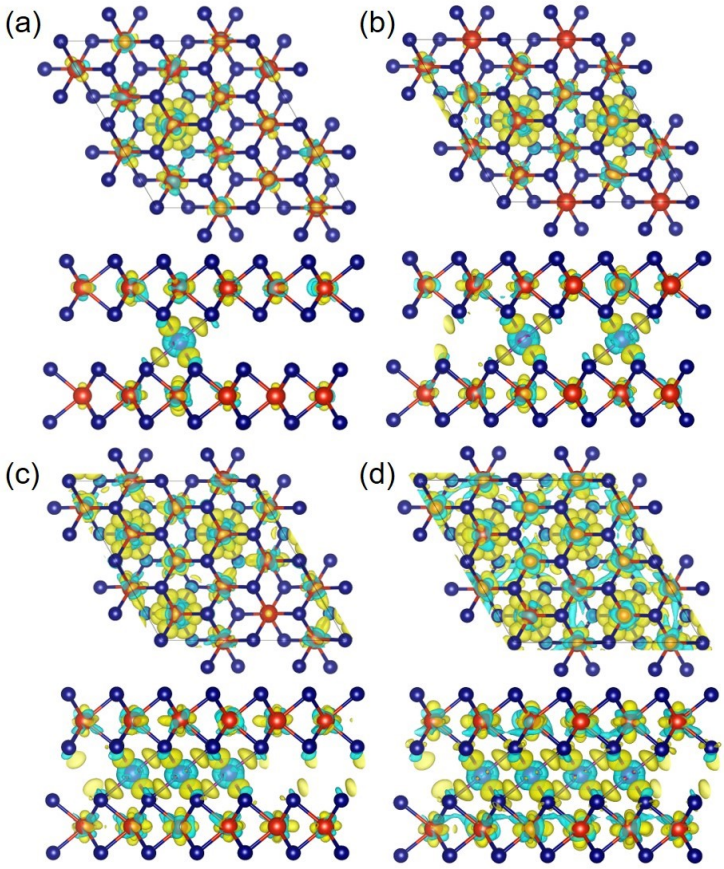

Fig. S5 The charge density difference of Cr-VS_2 with concentrations of (a) 8.3%, (b) 16.7%, (c) 25%, (d) 33.3%. The isosurface value is set at 0.005 e/Å^3. The blue and yellow regions represent charge depletion and accumulation, respectively.

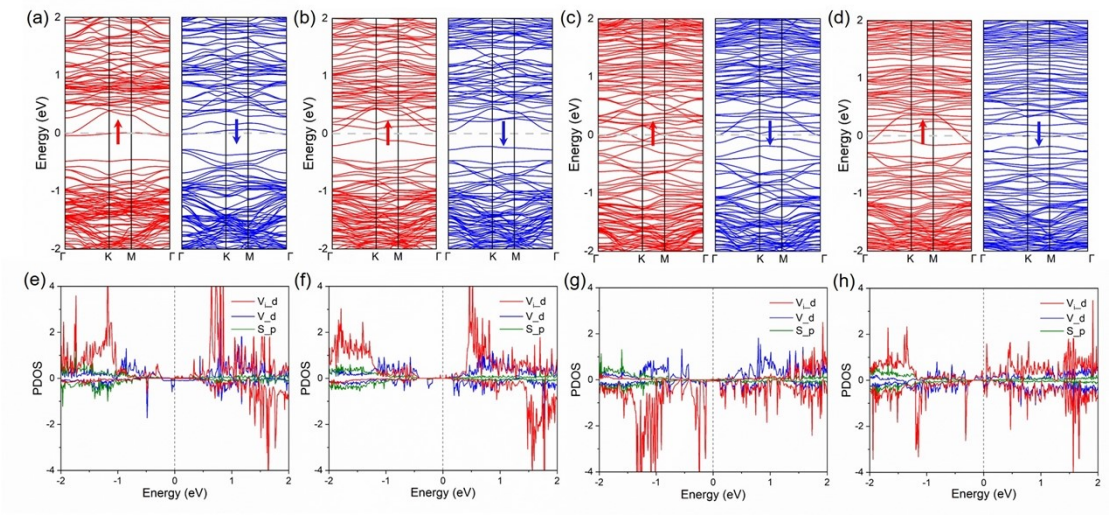

Fig. S6 (a-d) The spin-polarized band structures and (e-f) PDOS of V_i_d, V_d, S_p orbitals of V-VS_2 systems at the intercalation concentrations of 8.3%, 16.7%, 25%, 33.3%, respectively.

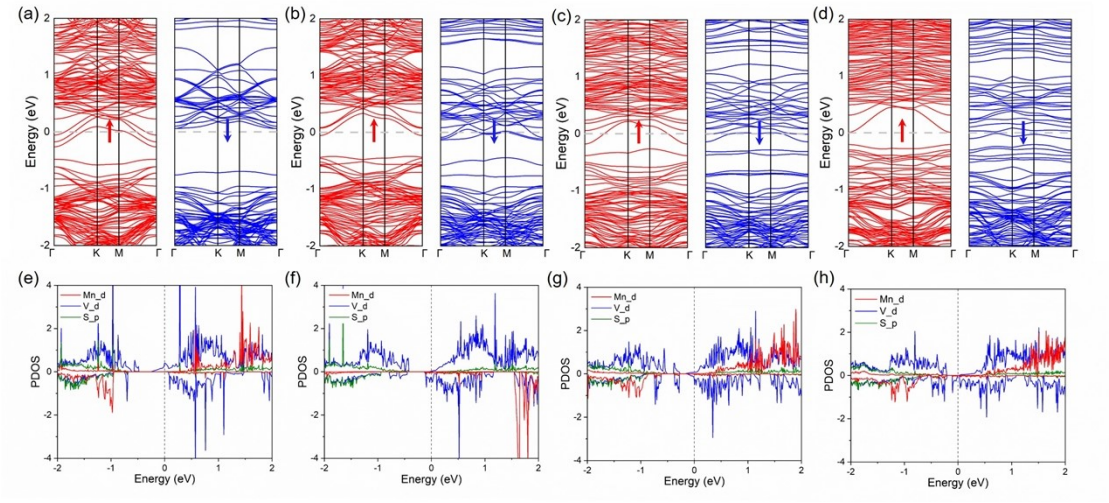

Fig. S7 (a-d) The spin-polarized band structures and (e-f) PDOS of Mn_d, V_d, S_p orbitals of Mn-VS_2 systems at the intercalation concentrations of 8.3%, 16.7%, 25%, 33.3%, respectively.

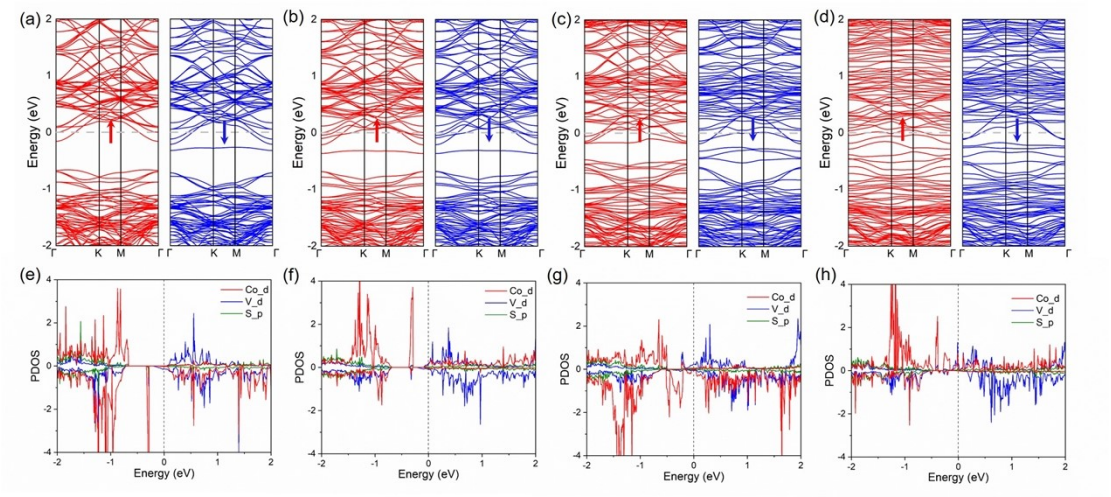

Fig. S8 (a-d) The spin-polarized band structures and (e-f) PDOS of Co_d, V_d, S_p orbitals of Co-VS_2 systems at the intercalation concentrations of 8.3%, 16.7%, 25%, 33.3%, respectively.

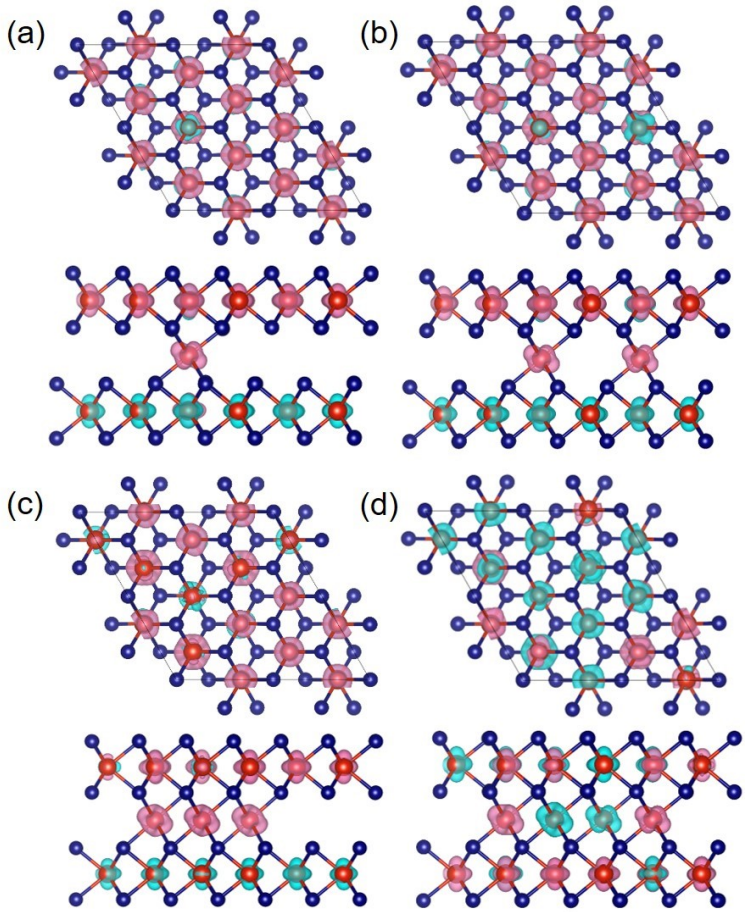

Fig. S9 Top and side views of spin density of V-VS_2 at the intercalation concentrations of (a) 8.3%, (b) 16.7%, (c) 25%, (d) 33.3%.

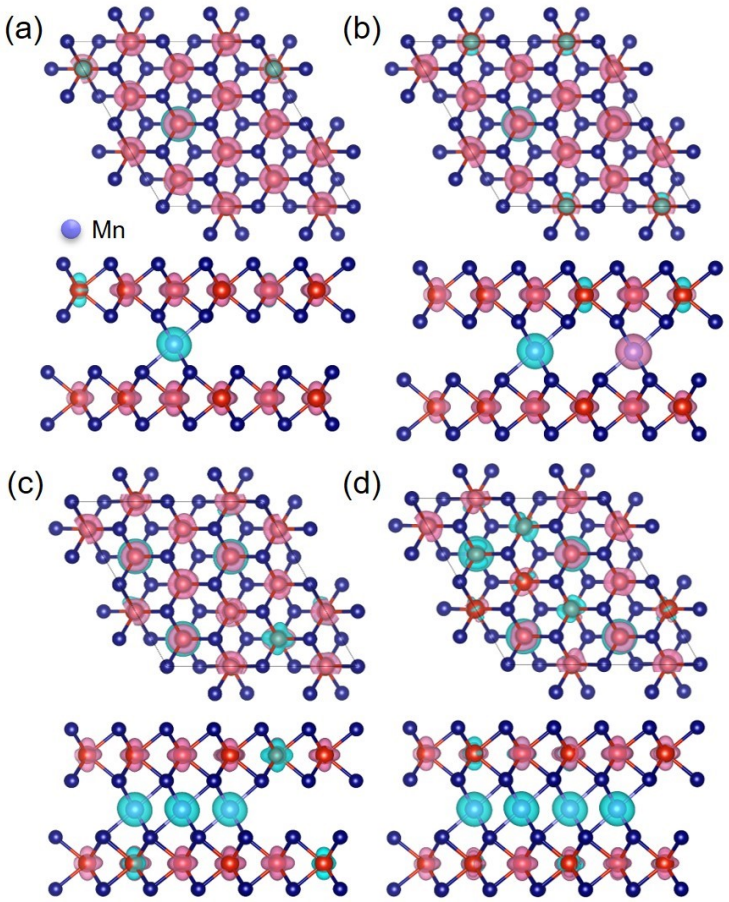

Fig. S10 Top and side views of spin density of Mn-VS_2 at the intercalation concentrations of (a) 8.3%, (b) 16.7%, (c) 25%, (d) 33.3%.

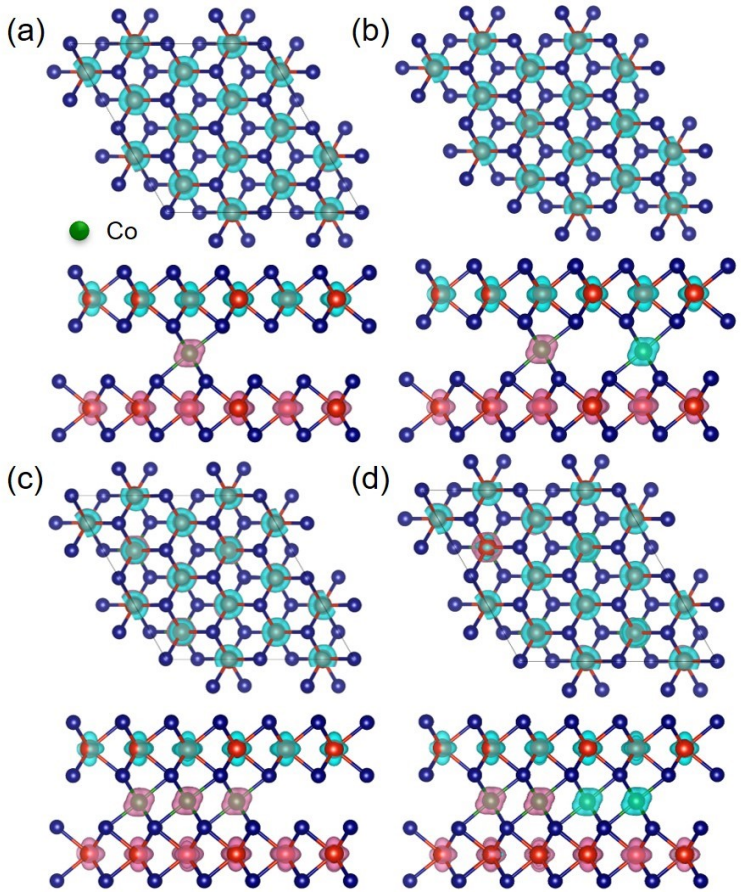

Fig. S11 Top and side views of spin density of Co-VS_2 at the intercalation concentrations of (a) 8.3%, (b) 16.7%, (c) 25%, (d) 33.3%.

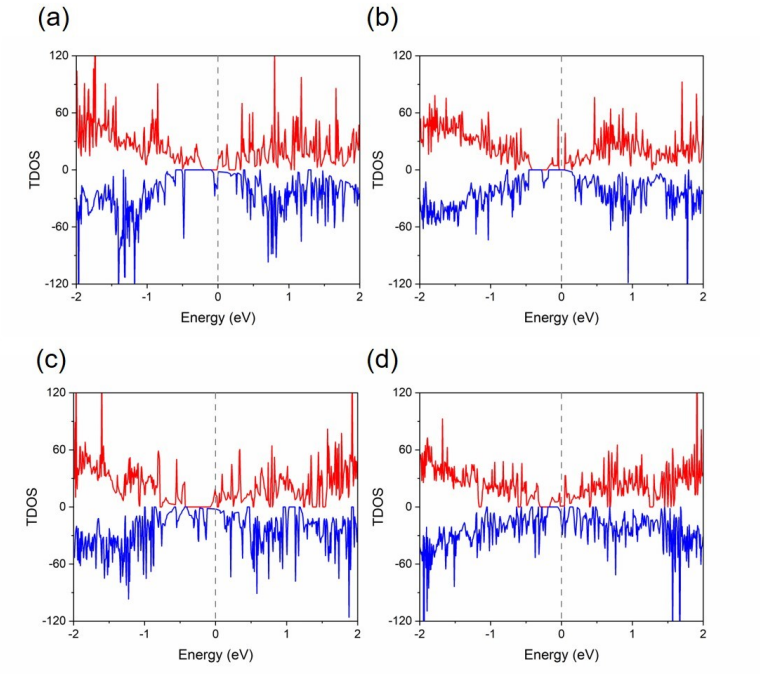

Fig. S12 (a-d) The TDOS of V-VS_2 systems at the intercalation concentrations of 8.3%, 16.7%, 25%, 33.3%, respectively. They correspond to ferromagnetic metal, ferromagnetic semiconductor, ferromagnetic metal, and antiferromagnetic metal, respectively.

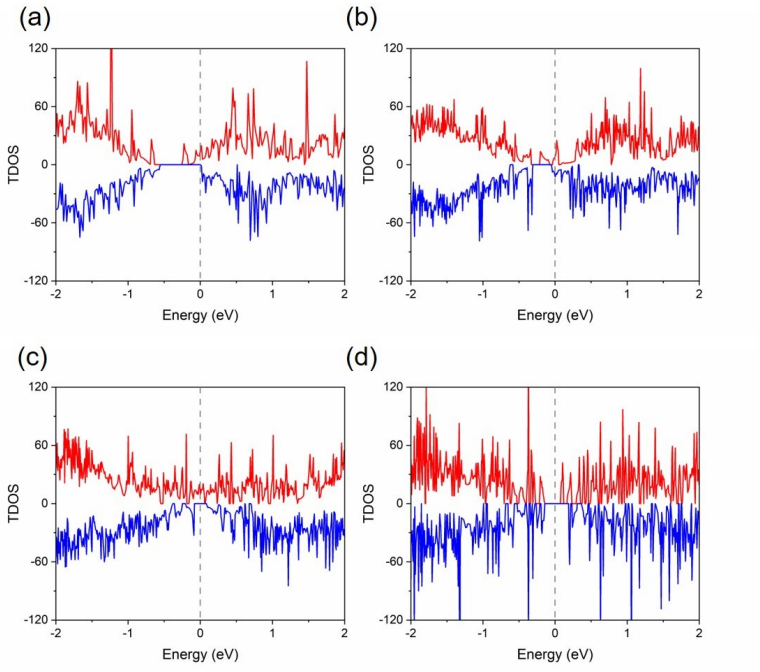

Fig. S13 (a-d) The TDOS of Cr-VS_2 systems at the intercalation concentrations of 8.3%, 16.7%, 25%, 33.3%, respectively. They correspond to ferromagnetic half-metal, antiferromagnetic metal, ferromagnetic half-metal, and antiferromagnetic semiconductor, respectively.

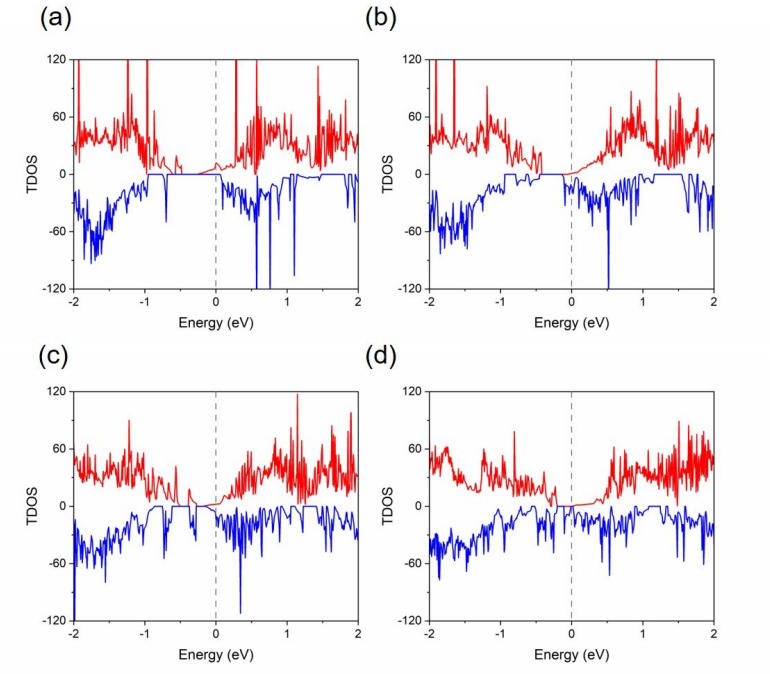

Fig. S14 (a-d) The TDOS of Mn-VS_2 systems at the intercalation concentrations of 8.3%, 16.7%, 25%, 33.3%, respectively. They correspond to ferromagnetic half-metal, antiferromagnetic metal, ferromagnetic metal, and ferromagnetic semiconductor, respectively.

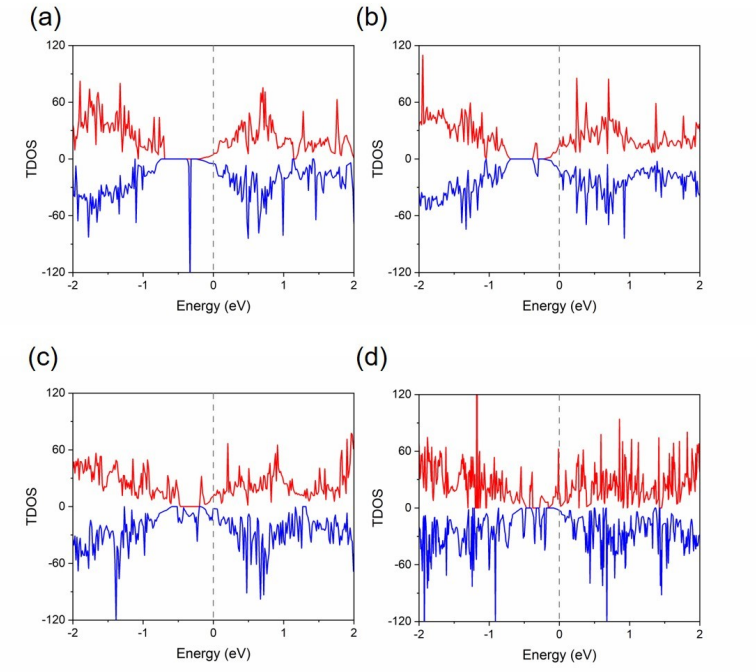

Fig. S15 (a-d) The TDOS of Co-VS_2 systems at the intercalation concentrations of 8.3%, 16.7%, 25%, 33.3%, respectively. They correspond to ferromagnetic metal, antiferromagnetic metal, ferromagnetic metal, and antiferromagnetic metal, respectively.

Table R1. Total energies (eV) of A-C configurations.

configuration	A	B	C
E (eV)	-427.52	-425.96	-427.21